Anomalous High-Temperature Magnetoresistance in a Dilute 2D Hole System

Arvind Shankar Kumar, Chieh-Wen Liu, Shuhao Liu, and Xuan P. A. Gao*
Department of Physics, Case Western Reserve University, 2076 Adelbert Road, Cleveland, Ohio 44106, USA

Alex Levchenko
Department of Physics, University of Wisconsin-Madison, Madison, Wisconsin 53706, USA

Loren N. Pfeiffer and Kenneth W. West
Department of Electrical Engineering, Princeton University, Princeton, New Jersey 08544, USA

(Received 4 April 2022; revised 15 August 2022; accepted 2 June 2023; published 26 June 2023)

We report an unusual magnetoresistance that strengthens with the temperature in a dilute two-dimensional (2D) hole system in GaAs/AlGaAs quantum wells with densities $p = 1.98 - 0.99 \times 10^{10}/\mathrm{cm}^2$ where r_s, the ratio between Coulomb energy and Fermi energy, is as large as 20–30. We show that, while the system exhibits a negative parabolic magnetoresistance at low temperatures ($\lesssim 0.4$ K) characteristic of an interacting Fermi liquid, a positive magnetoresistance emerges unexpectedly at higher temperatures, and grows with increasing temperature even in the regime $T \sim E_F$, close to the Fermi energy. This unusual positive magnetoresistance at high temperatures can be attributed to the viscous transport of 2D hole fluid in the hydrodynamic regime where holes scatter frequently with each other. These findings give insight into the collective transport of strongly interacting carriers in the $r_s \gg 1$ regime and new routes toward magnetoresistance at high temperatures.

DOI: 10.1103/PhysRevLett.130.266302

Magnetoresistance (MR)—the change in a material's resistivity with the application of a magnetic field—is one of the most basic tools to probe the quantum nature of materials, which is also of crucial importance to device applications in the form of magnetic sensors [1,2], magnetic memory [3], and energy-efficient computing [4,5]. It is also an important fundamental probe of material properties, and has been essential in the discoveries of integer and fractional quantum Hall effects [6,7], spin Hall effect [8], Aharanov-Bohm effect [9], weak localization and antilocalization effects [10], and many more. It can also be used to investigate the Fermi liquid (FL) nature of electronic materials—e.g., in the FL paradigm, a negative parabolic MR is expected when a perpendicular magnetic field B is applied to an interacting 2D electronic system at low temperatures [11–14], due to electron-electron (EE) or hole-hole (HH) interactions. This has subsequently been observed in many 2D electronic systems such as GaAs/AlGaAs heterostructures [15,16] and more recently in 2D materials like InSe [17] and epitaxial graphene [18], further lending to the success and ubiquity of FL theory. However, as temperature increases, all these quantum MR effects disappear.

Recently, FL analysis of carrier transport has been extended to the so-called hydrodynamic regime, where quasiparticles interact with each other more frequently than with phonons, impurities, or the sample boundaries [19–25]. In this case, the frequent EE/HH collisions have been shown to create collective behavior that is analogous to a classical viscous fluid. Signatures of viscous behavior in electron and hole transport and their effect on MR has been a popular direction of current research in different Dirac electron systems in which the disorder-limited carrier mean free path is very long such that the hydrodynamic regime can be accessed [20,22,26–31].

For 2D electron systems (2DES) or 2D hole systems (2DHS), the interaction effects are expected to be strong in the low-density regime since in 2D, $r_s = 1/(a^*\sqrt{\pi p})$ with p as the electron or hole density and $a^* = \hbar^2\epsilon/m^*e^2$ as the effective Bohr radius. Thanks to the tunable carrier density, and thus interaction strength, low-density 2DES/2DHS in semiconductor heterointerfaces with high mobilities have attracted great interest in studying strong Coulomb interactions induced phase transitions and breakdown of FL phases [32–39]. For example, in the discussions of the metal-insulator transition in 2D systems with high r_s [40], the applicability of conventional Boltzmann transport of FL has been challenged and new transport mechanisms like hydrodynamic transport have been suggested [19,41].

In this Letter, we find an unusual positive MR that increases with temperature in a strongly correlated 2DHS with $r_s \sim 20$–30, in a high-temperature regime where the conventional quantum transport effects of FL have been suppressed. We further find this MR to be consistent with predictions of viscous MR in the hydrodynamic regime. Our results give new insight into the FL transport theory in

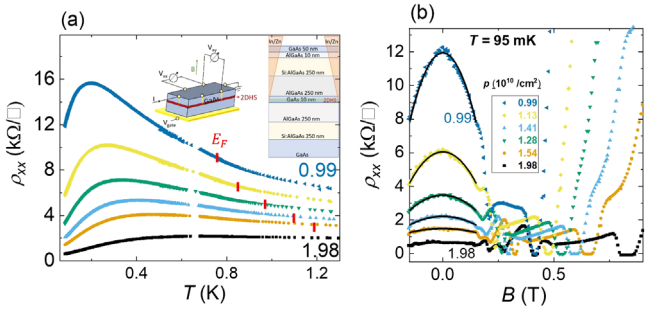

FIG. 1. (a) $\rho_{xx}(T)$ versus temperature T for the 2DHS confined in QW, plotted for various hole densities p listed in the figure, in the range 0.99–1.98 $\times 10^{10}/\mathrm{cm}^2$ [values listed in (b)]. Values of E_F (in units of k_B) for each density are marked in red on the curves. Inset: GaAs/AlGaAs 10 nm QW device structure (side view) and device schematic. (b) $\rho_{xx}(T)$ versus magnetic field B, applied perpendicular to the 2DHS plane, at $T = 95$ mK for the densities listed in the figure. Black solid lines correspond to fits to the B^2 dependence.

strongly correlated 2D electronic systems and also provide a new possible route to high-temperature MR.

Our experiments were performed on the modulation-doped p-type GaAs quantum wells (QWs) with 10 nm thickness. The samples were grown on (100) GaAs wafer (samples 1–3) or (311) GaAs wafer (sample 4) with $Al_{0.1}Ga_{0.9}As$ barriers and symmetrically placed Si delta doping layer 200 nm away from the QW, creating a high mobility, low-density 2DHS in the GaAs QW [see Fig. 1(a) for device structure]. The hole density of the samples without gating was $p \sim 2$ (for this Letter, hole densities are in units of $10^{10}/\mathrm{cm}^2$) and the low-temperature mobility was $\mu \sim 1$–2×10^5 $\mathrm{cm}^2/\mathrm{Vs}$ over the density range explored. The carrier density is tuned ($p \sim 1$–2) using a back gate placed approximately 150 μm away from the 2DHS, so that screening of Coulomb interactions due to the back gate is negligible (see Methods section for further fabrication and measurement details [42]). The samples are cut into 3 mm wide Hall bars with an effective length defined by longitudinal voltage contacts that are separated by ∼5 mm.

In Fig. 1(a), we plot the temperature-dependent resistivity $\rho_{xx}(T)$ for our 2DHS sample (for clarity, all data presented in the main text are from sample 1 except where explicitly stated). We observe a nonmonotonic behavior that crosses over from insulatinglike behavior at high temperatures to metallic behavior at low temperatures. This sign change in $\partial\rho/\partial T$ has been previously observed over this density range in samples of similar mobility [33,40,51] and was a subject of active discussion in the context of 2D metal-insulator transition [40,41]. Figure 1(b) shows longitudinal magnetoresistivity $\rho_{xx}(B)$—the focus of our study—at 95 mK where, in addition to dips corresponding to quantum Hall states at higher perpendicular magnetic field B, we observe a clear negative parabolic MR at $B \lesssim 0.2$ T over the entire density range. The temperature evolution of the observed parabolic MR in Fig. 1(b) is plotted for different densities and additional samples are plotted in Figs. S2 and S3 in Supplemental Material (SM) [42].

While the Drude model of noninteracting electrons predicts zero MR, a B-independent correction $\delta\sigma$ to the longitudinal Drude conductivity combined with the Drude magnetoconductivity, which has a $1/[1 + (\mu B)^2]$ dependence, will lead to a parabolic MR whose magnitude is determined by $\delta\sigma$ as given by

$$\rho_{xx} = \frac{1}{\sigma_0}\left[1 - [1 - (\omega_c\tau)^2]\frac{\delta\sigma}{\sigma_0}\right]. \quad (1)$$

In the interaction correction theories of FL [11,13,14,52], negative parabolic MR behavior are often attributed to the interaction correction $\delta\sigma$. Although for our system with $r_s \gg 1$, it is not clear that interaction effects can be treated as perturbative corrections, we can still extract a correction $\delta\sigma$ to the conductivity according to Eq. (1) from the observed parabolic MR data and compare to relevant theories. The extracted $\delta\sigma$ from the observed negative parabolic MR are plotted versus temperature T for various densities in Fig. 2. Note that during the fitting process, $\delta\sigma$ is the only parameter fitted from the curvature of the B^2 dependent $\rho_{xx}(B)$ at a given T after we substitute $\omega_c\tau$ with μB and σ_0 with $pe\mu$ which cancels the unknown μ or τ. We observe that $\delta\sigma(T)$ gives a negative correction that tends to make the system more insulating, and the magnitude of the correction increases as we lower the density. Also, the T dependence of the correction $\delta\sigma(T)$ seems to follow the $\ln T$ dependence at lower temperatures (Fig. 2) and diminishes toward zero as T increases (inset of Fig. 2),

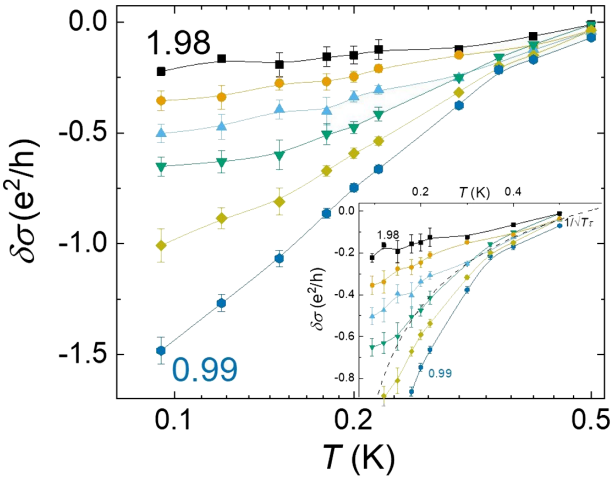

FIG. 2. Correction to the conductivity $\delta\sigma(T)$ extracted from the MR data using Eq. (1), plotted versus temperature for the densities (from top) $p = 1.98, 1.54, 1.41, 1.28, 1.13, 0.99$. Inset: $\delta\sigma(T)$ data enlarged to show the high temperature range and plotted in linear scale. Dashed line corresponds to fit to $1/\sqrt{T\tau}$ dependence for the $p = 1.41$ over the $T \geq 0.3$ K range.

qualitatively similar to the expectations of interaction corrections in the FL theory [13,43,52]. However, the negative sign (and insulatinglike nature) of $\delta\sigma(T)$ is opposite to the strong metallic trend of the system within this temperature range. Moreover, a detailed analysis of $\delta\sigma(T)$ and Hall data using FL theories covering both diffusive and ballistic regimes (see Methods section in SM [42]) yields unphysical behavior of the FL parameter F_0^σ (see Figs. S4, S5 in SM [42]) despite the fact that the T dependence may be described by the $\ln T$ and $1/\sqrt{T}$ behavior as the FL interaction correction theories expect [13,43]. We conclude that although the FL interaction corrections can explain the negative parabolic MR at low temperatures, it is not the dominant cause for the overall metallic conductivity of the system at low T.

In light of this, we plot $\sigma - \delta\sigma$ versus T, in Fig. 3 to examine the behavior of the system's raw conductivity without the correction part. The raw conductivity shows a strong metallic temperature dependence at low temperatures ($T \lesssim 0.4$ K), which cannot be attributed to quantum corrections as discussed above. Classical single-particle scattering effects like hole-phonon scattering is also not relevant in this temperature and density range (see Fig. S6 in SM [42] for scattering length calculations). In fact, at the lowest density $p = 0.99$, we see that $\delta\sigma$ constitutes a relatively large fraction (~30%–40%) of the conductivity at the lowest temperature, but this fraction consistently reduces at higher density when the system is more metallic and is close to zero at $p = 1.98$. At the same time, at high temperatures (~0.4–1 K) where the quantum correction effects are essentially absent, the system exhibits an unusual insulatinglike temperature dependence [also see the data showing decreasing resistivity at high T in Fig. 1(a)]. In this regime, since the system's carrier density is low and temperature $T \sim E_F$—the Fermi energy (in units of k_B)—it was speculated that the increasing σ or decreasing ρ with T is due to the T-dependent viscosity of a correlated fluid in the "semiquantum" regime, in analogy to helium-3 fluid at $T \sim E_F$ [44]. Yet there has been no further experimental test of this idea of understanding the transport in a high r_s 2D system using hydrodynamics which we address below.

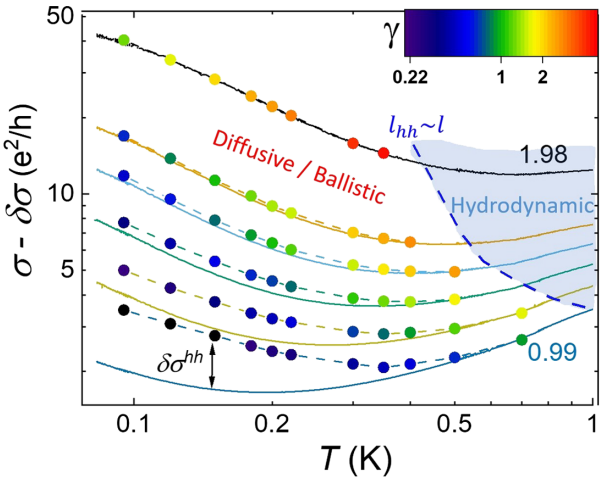

FIG. 3. $\sigma - \delta\sigma$, conductivity without the correction term, plotted versus T for the densities listed in Figs. 1 and 2. The color of each point indicates $\gamma = (k_B T/\hbar/\tau)$ values, as shown in the inset color map, and color of the dashed line along the points indicates corresponding density values as in Fig. 2. The solid lines are a plot of measured σ vs T for the corresponding densities [same data as in Fig. 1(a)]. The blue dashed line indicates the temperature above which $l_{\mathrm{HH}} < l$ for the respective curves and the shaded region indicates the corresponding hydrodynamic transport regime where Drude conductivity with corrections no longer applies (see Methods section in SM [42]).

In conducting materials, the electronic hydrodynamic transport regime is typically seen at relatively high temperatures, where the quasiparticle-quasiparticle scattering length (HH scattering in our case) l_{HH} is shorter than the mean free path l due to momentum-relaxing collisions (e.g., with impurities, phonons, etc.) [19,41]. Interestingly, for our strongly correlated 2DHS system with high mobility, we find that the criterion $l_{\mathrm{HH}} < l$ is satisfied at $T > 0.4$ K, where σ increases with T, as marked in Fig. 3 (further discussion of l_{HH} and l in SM, Fig. S6 [42]). Surprisingly, in the high-T regime, we find that the MR does not disappear as in the standard classical Drude theory which predicts zero MR. Instead, a positive MR emerges at low B and grows stronger as T increases and this positive MR also appears to follow a parabolic B dependence as shown in Fig. 4(a) for $p = 1.54$ and $p = 0.99$. Remarkably, the positive MR in the hydrodynamic regime keeps increasing with temperature even at temperatures

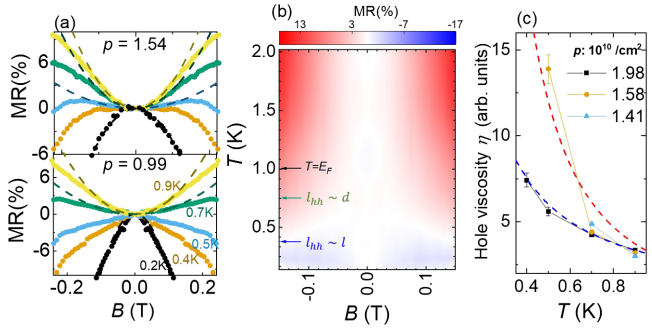

FIG. 4. (a) MR [$= \Delta\rho(B)/\rho(0)$ (%)] versus B at $p = 1.54$ (top) and $p = 0.99$ (bottom) plotted for $T = 0.2$–0.9 K. Dashed lines are fits to B^2 dependence of low-field data (-0.1 T $< B < 0.1$ T) for corresponding temperatures. (b) Color plot of MR(%) versus B and T (for sample 4 at $p = 1.13$) up to $T = 2$ K. Blue and green arrows indicate temperatures above which $l_{\mathrm{HH}} \lesssim l$ and $l_{\mathrm{HH}} \lesssim d$, respectively, and the black arrow marks $T = E_F$. (c) Temperature dependence of hole viscosity—extracted from fitting the MR at high T as in (a) using Eq. (2), at different hole densities listed in figure. The solid lines are a guide to the eye. Blue and red dashed lines correspond to $\eta \propto (1/T)$ and $\eta \propto (1/T^2)$ dependencies, respectively.

higher than the Fermi temperature, as shown in Fig. 4(b) for $p = 1.13$ in a different sample. (The switching from negative MR to positive parabolic MR in the hydrodynamic regime at high T was observed for all the carrier densities studied. Additional data can be seen in Figs. S3, and S7, S8 in SM [42]).

A MR that grows stronger with increasing temperature is unusual, especially in the regime $T \sim E_F$ where the classical Drude behavior (i.e., zero MR) is expected [the estimated Fermi energy is marked on Fig. 1(a) for different densities]. To understand this, we therefore consider a contribution to conductivity and MR from the viscous fluidlike transport of holes in the hydrodynamic regime. In a recent theoretical model [23], it was predicted that such viscosity effects in a 2DES/2DHS with long-range disorder lead to a positive parabolic MR, whose temperature dependence is due to the temperature dependence of the viscosity of the electron or hole fluid. This regime occurs above a characteristic temperature determined from the condition $l_{\mathrm{HH}}(T) \lesssim d$, where d is the distance to the dopant-spacer layer, that marks the onset of hydrodynamic behavior. The predicted MR has the form (in units $\hbar = c = 1$)

$$\rho = \rho_0(T) + \frac{\ln(L/d)}{2p\eta(T)} B^2, \tag{2}$$

where $L \gg \{l, 1/k_F\}$ is a large spacial length scale, $\rho_0(T)$ is the field-independent component of resistivity, and $\eta(T)$ is the hole viscosity. The temperature evolution of the hole viscosity can hence be extracted from the positive parabolic MR in the high-T hydrodynamic regime, seen in Fig. 4(a) for $p = 1.54$ and $p = 0.99$, using Eq. (2) (data from other densities and sample are plotted in Figs. S7 and S8 in SM [42]). In Fig. 4(b), we see that the onset of this positive hydrodynamic MR coincides with the temperature range where $l_{\mathrm{HH}} \sim l$—marked by the blue arrow ($l_{\mathrm{HH}} \sim d$ is also marked in the figure). Additionally, we also see from this figure that this positive MR continues to grow in the regime where $T > E_F$, contrary to classical Drude MR or FL interaction correction (see Fig. S8 in SM [42] for further details). In Fig. 4(c), we plot the extracted hole viscosity at a few different densities for the main sample discussed in the Letter (similar trend of the viscosity for sample 4 is presented in Fig. S9 in [42] where the sample was only measured at a fixed density without gating).

Figure 4(c) shows a decreasing trend in the temperature dependence of hole viscosity (a similar trend was also observed over a larger temperature range in an additional sample—see Figs. S8 and S9 in SM [42]). This T dependence of viscosity extracted from the hydrodynamic MR alone without using other information follows the insulatinglike decreasing $\rho(T)$ over this high-temperature range, as seen in Fig. 1(a) as well as Fig. S1 in SM [42], and is thus consistent with the viscosity explanation [44] for this puzzling insulatinglike temperature dependent $\rho(T)$ of high-mobility 2D carriers with large r_s in the semiquantum regime where the temperature is high. Within the hydrodynamic description of transport one expects viscosity $\eta(T) \propto 1/T^2$ and $\eta(T) \propto 1/T$ in the $T < E_F$ and $T > E_F$ regimes, respectively (see Method section in SM [42]). Our extracted viscosity follows $\propto 1/T^b$ with $1 < b < 2$ and is consistent with the fact that the temperature range where the hydrodynamic MR emerges spans both $T < E_F$ and the semiquantum regime $T \sim E_F$. The physical mechanism for the decreasing temperature dependence of resistivity ($\partial\rho/\partial T < 0$) in a viscous electron or hole fluid is known as the Gurzhi effect and is a prominent signature of hydrodynamic behavior in conducting systems [26,53]. It has been observed in electrons in graphene, where a temperature dependence of electron viscosity similar to in Fig. 4(c) has been shown to agree with predictions of many-body theory [54]. In our low-density 2D system, it is known that $\rho(T) \propto 1/T$ in the semiquantum regime $T \sim E_F$ [51], again consistent with the $\rho(T)$ being dominated by the viscosity effect with $\eta(T) \propto 1/T$ in this temperature regime.

To summarize, the data in Fig. 2 are a signature of magnetic field independent correction to the conductivity of our $r_s \gg 1$ 2DHS at low temperatures, as anticipated in the standard FL theory of interaction corrections. However, the behavior of extracted conductivity correction contradicts the overall metallic conductivity behavior over this temperature range (Fig. 3) and does not result in a consistent F_0^σ prediction. Interestingly, at higher temperatures, we also observe the emergence of a positive MR that increases with T [seen clearly in Fig. 4(b) up to the $T > E_F$ regime], contrary to conventional MR which becomes weaker at higher T. In Fig. 4—along with the corresponding discussion—we see a resolution of this novel positive MR, along with the insulatinglike $\rho(T)$ at the higher temperature, through the consideration of viscous MR in the hydrodynamic regime, according to Ref. [23]. Therefore, we believe that we have reached a consistent picture for both the unusual decreasing $\rho(T)$ and positive MR in the high T regime through the hydrodynamic viscosity effect. The unusual hydrodynamic MR that becomes stronger at higher temperatures reported here opens the door to a new way of understanding magnetotransport phenomena and inducing magnetoresistance at high temperatures in strongly correlated electronic systems.

The authors thank Anton Andreev, Steven Kivelson, and Boris Spivak for fruitful discussions and prior collaboration on related topics. X. P. A. G. acknowledges the financial support from NSF (Grant No. DMR-1607631). The work of A. L. at UW-Madison was supported by the National Science Foundation Grants No. DMR-1653661 and No. DMR-2203411 and H. I. Romnes Faculty Fellowship provided by the University of Wisconsin-Madison Office of the Vice Chancellor for Research and

Graduate Education with funding from the Wisconsin Alumni Research Foundation. The work at Princeton was partially funded by the Gordon and Betty Moore Foundation and the NSF MRSEC Program through the Princeton Center for Complex Materials (No. DMR-0819860).

*Corresponding author.
xuan.gao@case.edu

[1] C. Reig, M.-D. Cubells-Beltrán, and D. Ramírez Muñoz, Sensors **9**, 7919 (2009).
[2] M. Djamal and Ramli, Proc. Eng. **32**, 60 (2012).
[3] S. Bhatti, R. Sbiaa, A. Hirohata, H. Ohno, S. Fukami, and S. Piramanayagam, Mater. Today **20**, 530 (2017).
[4] J. A. Currivan-Incorvia, S. Siddiqui, S. Dutta, E. R. Evarts, J. Zhang, D. Bono, C. A. Ross, and M. A. Baldo, Nat. Commun. **7**, 10275 (2016).
[5] J. Lee, D. I. Suh, and W. Park, J. Appl. Phys. **117**, 17D717 (2015).
[6] K. von Klitzing, T. Chakraborty, P. Kim, V. Madhavan, X. Dai, J. McIver, Y. Tokura, L. Savary, D. Smirnova, A. M. Rey, C. Felser, J. Gooth, and X. Qi, Nat. Rev. Phys. **2**, 397 (2020).
[7] H. L. Stormer, D. C. Tsui, and A. C. Gossard, Rev. Mod. Phys. **71**, S298 (1999).
[8] S. O. Valenzuela and M. Tinkham, Nature (London) **442**, 176 (2006).
[9] D. Y. Sharvin and Y. V. Sharvin, JETP Lett. **34**, 285 (1981).
[10] G. Bergmann, Phys. Rep. **107**, 1 (1984).
[11] A. Houghton, J. R. Senna, and S. C. Ying, Phys. Rev. B **25**, 2196 (1982).
[12] B. Altshuler and A. Aronov, in *Electron-Electron Interactions in Disordered Systems*, Modern Problems in Condensed Matter Sciences Vol. 10, edited by A. Efros and M. Pollak (Elsevier, New York, 1985), pp. 1–153.
[13] I. V. Gornyi and A. D. Mirlin, Phys. Rev. Lett. **90**, 076801 (2003).
[14] A. Levchenko, Phys. Rev. B **79**, 212511 (2009).
[15] L. Li, Y. Y. Proskuryakov, A. K. Savchenko, E. H. Linfield, and D. A. Ritchie, Phys. Rev. Lett. **90**, 076802 (2003).
[16] L. Bockhorn, P. Barthold, D. Schuh, W. Wegscheider, and R. J. Haug, Phys. Rev. B **83**, 113301 (2011).
[17] A. S. Kumar, K. Premasiri, M. Gao, U. R. Kumar, R. Sankar, F.-C. Chou, and X. P. A. Gao, Phys. Rev. B **102**, 121301(R) (2020).
[18] J. Jobst, D. Waldmann, I. V. Gornyi, A. D. Mirlin, and H. B. Weber, Phys. Rev. Lett. **108**, 106601 (2012).
[19] A. V. Andreev, S. A. Kivelson, and B. Spivak, Phys. Rev. Lett. **106**, 256804 (2011).
[20] J. Crossno, J. K. Shi, K. Wang, X. Liu, A. Harzheim, A. Lucas, S. Sachdev, P. Kim, T. Taniguchi, K. Watanabe, T. A. Ohki, and K. C. Fong, Science **351**, 1058 (2016).
[21] B. N. Narozhny, I. V. Gornyi, A. D. Mirlin, and J. Schmalian, Ann. Phys. (Berlin) **529**, 1700043 (2017).
[22] A. Lucas and K. C. Fong, J. Phys. Condens. Matter **30**, 053001 (2018).
[23] A. Levchenko, H.-Y. Xie, and A. V. Andreev, Phys. Rev. B **95**, 121301(R) (2017).
[24] I. Mandal and A. Lucas, Phys. Rev. B **101**, 045122 (2020).
[25] A. Levchenko and J. Schmalian, Ann. Phys. (Amsterdam) **419**, 168218 (2020).
[26] M. Polini and A. Geim, Phys. Today **73**, No. 6, 28 (2020).
[27] A. I. Berdyugin, S. G. Xu, F. M. D. Pellegrino, R. Krishna Kumar, A. Principi, I. Torre, M. Ben Shalom, T. Taniguchi, K. Watanabe, I. V. Grigorieva, M. Polini, A. K. Geim, and D. A. Bandurin, Science **364**, 162 (2019).
[28] J. A. Sulpizio, L. Ella, A. Rozen, J. Birkbeck, D. J. Perello, D. Dutta, M. Ben-Shalom, T. Taniguchi, K. Watanabe, T. Holder, R. Queiroz, A. Principi, A. Stern, T. Scaffidi, A. K. Geim, and S. Ilani, Nature (London) **576**, 75 (2019).
[29] P. J. W. Moll, P. Kushwaha, N. Nandi, B. Schmidt, and A. P. Mackenzie, Science **351**, 1061 (2016).
[30] J. Gooth, F. Menges, N. Kumar, V. Süß, C. Shekhar, Y. Sun, U. Drechsler, R. Zierold, C. Felser, and B. Gotsmann, Nat. Commun. **9**, 4093 (2018).
[31] A. Levchenko, S. Li, and A. V. Andreev, Phys. Rev. B **106**, L201306 (2022).
[32] S. V. Kravchenko, G. V. Kravchenko, J. E. Furneaux, V. M. Pudalov, and M. D'Iorio, Phys. Rev. B **50**, 8039 (1994).
[33] J. Yoon, C. C. Li, D. Shahar, D. C. Tsui, and M. Shayegan, Phys. Rev. Lett. **82**, 1744 (1999).
[34] R. L. J. Qiu, X. P. A. Gao, L. N. Pfeiffer, and K. W. West, Phys. Rev. Lett. **108**, 106404 (2012).
[35] T. Knighton, Z. Wu, V. Tarquini, J. Huang, L. N. Pfeiffer, and K. W. West, Phys. Rev. B **90**, 165117 (2014).
[36] J. Huang, L. Pfeiffer, and K. West, Appl. Sci. **9**, 80 (2018).
[37] P. Brussarski, S. Li, S. V. Kravchenko, A. A. Shashkin, and M. P. Sarachik, Nat. Commun. **9**, 3803 (2018).
[38] A. A. Shashkin and S. V. Kravchenko, Appl. Sci. **9**, 1169 (2019).
[39] J. Jang, B. M. Hunt, L. N. Pfeiffer, K. W. West, and R. C. Ashoori, Nat. Phys. **13**, 340 (2017).
[40] E. Abrahams, S. V. Kravchenko, and M. P. Sarachik, Rev. Mod. Phys. **73**, 251 (2001).
[41] B. Spivak, S. V. Kravchenko, S. A. Kivelson, and X. P. A. Gao, Rev. Mod. Phys. **82**, 1743 (2010).
[42] See Supplemental Material at http://link.aps.org/supplemental/10.1103/PhysRevLett.130.266302 for experimental and theoretical methods and further supplemental low-temperature magnetotransport characterization data and data from additional samples; Refs. [11,13,15,19,23,41,43–50] are cited therein.
[43] G. Zala, B. N. Narozhny, and I. L. Aleiner, Phys. Rev. B **64**, 214204 (2001).
[44] B. Spivak and S. Kivelson, J. Phys. IV (France) **131**, 255 (2005).
[45] Y. Y. Proskuryakov, A. K. Savchenko, S. S. Safonov, M. Pepper, M. Y. Simmons, and D. A. Ritchie, Phys. Rev. Lett. **89**, 076406 (2002).
[46] H. Noh, M. P. Lilly, D. C. Tsui, J. A. Simmons, E. H. Hwang, S. Das Sarma, L. N. Pfeiffer, and K. W. West, Phys. Rev. B **68**, 165308 (2003).

[47] J. Eisenstein, D. Syphers, L. Pfeiffer, and K. West, Solid State Commun. **143**, 365 (2007).
[48] M. Roger, Phys. Rev. B **30**, 6432 (1984).
[49] M. P. Jura, M. Grobis, M. A. Topinka, L. N. Pfeiffer, K. W. West, and D. Goldhaber-Gordon, Phys. Rev. B **82**, 155328 (2010).
[50] V. Karpus, Semicond. Sci. Technol. **5**, 691 (1990).
[51] N. J. Goble, J. D. Watson, M. J. Manfra, and X. P. A. Gao, Phys. Rev. B **90**, 035310 (2014).
[52] B. Altshuler and A. Aronov, Solid State Commun. **46**, 429 (1983).
[53] M. J. M. de Jong and L. W. Molenkamp, Phys. Rev. B **51**, 13389 (1995).
[54] R. Krishna Kumar, D. A. Bandurin, F. M. D. Pellegrino, Y. Cao, A. Principi, H. Guo, G. H. Auton, M. Ben Shalom, L. A. Ponomarenko, G. Falkovich, K. Watanabe, T. Taniguchi, I. V. Grigorieva, L. S. Levitov, M. Polini, and A. K. Geim, Nat. Phys. **13**, 1182 (2017).